Original Research

Toxicological profile of small airway epithelial cells exposed to gold nanoparticles

Cheng-Teng Ng[1,2], Jasmine Jia'En Li[1,2], Resham Lal Gurung[3], Manoor Prakash Hande[3], Choon-Nam Ong[4], Boon-Huat Bay[1] and Lin-Yue Lanry Yung[2]

[1]Department of Anatomy, Yong Loo Lin School of Medicine, National University of Singapore, S117597 Singapore; [2]Department of Chemical and Biomolecular Engineering, National University of Singapore, S117576 Singapore; [3]Department of Physiology, Yong Loo Lin School of Medicine, National University of Singapore, S117597 Singapore; [4]Saw Swee Hock School of Public Health, National University of Singapore, S117597 Singapore

Corresponding authors: Boon-Huat Bay. Email: boon_huat_bay@nuhs.edu.sg or; Lin-Yue Lanry Yung. Email: cheyly@nus.edu.sg

Abstract

Gold nanoparticles (AuNPs) have diverse applications in the biomedical industry such as in diagnosis, labeling, delivering and sensing. Despite their prevalent medical use, nanotoxicity induced by AuNPs is still largely unknown. We have previously shown that AuNPs could exert cytotoxic effects on lung fibroblasts. In this study, we investigated the *in vitro* toxicological effects of AuNPs in small airway epithelial cells (SAECs) which are the first cells of contact for inhaled NPs and compared expression of metallothionein (MT), a reactive oxygen species scavenger, in SAECs and lung fibroblasts *in vitro*. Transmission electron microscopy (TEM) and energy-dispersive X-ray (EDX) spectroscopy study revealed cellular uptake of aggregates of AuNPs into the cytoplasm at the ultrastructural level. A significant increase in lipid peroxide as well as substantial DNA damage and cytotoxicity was observed in AuNP-treated cells. For *MT* expression, AuNPs induced down-regulation of the *MT-1X* isoform in SAECs, but up-regulation of the *MT-1X* and *MT-2A* isoforms in MRC5 lung fibroblasts. The present study suggests that AuNPs could induce oxidative stress-related cytotoxicity and genotoxicity in SAECs.

Keywords: Gold nanoparticles, lung, cytotoxicity and genotoxicity, metallothionein (MT), oxidative stress, DNA damage

***Experimental Biology and Medicine* 2013; 238: 1355–1361. DOI: 10.1177/1535370213505964**

Introduction

Nanoparticles (NPs) are defined as particulate substances possessing at least one dimension less than 100 nm.[1,2] According to the US Environmental Protection Agency, engineered NPs can be categorized into four types, namely carbon-based materials, metal-based materials (quantum-dots, nanogold), polymeric dendrimers and composites.[3] They possess properties such as durability and high conductivity and high reactivity which have led to their applications in a wide range of products.[4,5] Up to this day, applications of engineered NPs have been extended to consumer products, electronic goods, food industry and biomedical area. For instance, gold nanoparticles (AuNPs) have diverse applications in drug and gene delivery, given their relatively good biocompatibility.[6,7] With an increasing ability to functionally control such materials and an estimate of $2.6 trillion for the sales of nanotechnology-associated products by 2014, a variety of nanomaterials are being developed for consumer and industrial application.[5,8]

Engineered NPs generally behave substantially different from their respective bulk materials of the same composition. Many studies have revealed that these NPs are more likely to be toxic as their small size, high surface to volume ratio and surface functionalities allow them to enter cells and cause unwanted biological responses such as genotoxicity.[9,10] For example, ultrafine particles like carbon nanotubes could, when inhaled, deposit in the alveolar region as opposed to larger particles that get trapped in the upper airway, thereby increasing risk of getting acute pulmonary toxicity and genotoxicity as demonstrated in animal models.[11,12] Exposure to NPs via inhalation is the primary route of entry and hence the lung is the first-line exposure organ to aerosolized NPs. The lung functions as a filter for NPs and is more likely a potential site for NPs deposition.[13] Nowadays, exposure to NPs not only occurs in consumer products, but also in the ambient air, for example, exposure to titanium dioxide NPs occurs mostly in the workplace during manufacturing process.[14–16] Hence, occupational health hazards of inhaled NPs are unavoidable.[17] Knowledge on the amount of NPs that reach the lungs

from inhalation is essential and this has led to toxicity studies using inhalation as the exposure route, since inhaled NPs may pose potential pulmonary toxicity.[18,19]

Various *in vitro* studies have also revealed that AuNPs are capable of generating oxidative stress in cells, resulting in toxicity and accounting for the main cause of cellular damage.[13,20,21] As nano-sized particles have higher reactivity, they are more likely to absorb endogenous substances, induce DNA damage and generate reactive oxygen species (ROS) that damage plasma membrane and evoke inflammatory responses, potentially initiating a series of toxic responses far from the initial site of deposition.[22] Current research suggests that exposure to NPs may impart various levels of cytotoxicity, depending on the size of NPs and route of exposure in the body.[18]

Metallothionein (MT) is an antioxidant with selective affinity for divalent essential metals, such as zinc, copper and non-essential metals such as mercury and cadmium.[23,24] MT has also been reported to bind Au following intraperitoneal injection in rats.[25] Since *MT* is a metal-responsive gene, it is likely that exposure of cells to AuNPs could modulate *MT* expression. We have also previously shown that AuNPs induce genomic instability, DNA damage and autophagy concomitant with oxidative stress in lung fibroblasts[13,26,27] This present study evaluated the toxic effects and modulation of MT expression due to AuNP exposure in human small airway epithelial cells (SAECs) *in vitro*. The results verified that AuNP induced lipid peroxidative stress and exerted both genotoxic and cytotoxic effects in SAECs. Differential modulation of the *MT* isoforms was observed when the *MT* isoforms were compared in SAECs as well as MRC5 lung fibroblasts following AuNP treatment.

Materials and methods

Cell culture

Primary human SAECs were cultured in small airway cells growth medium (SAGM). MRC5 lung fibroblasts were cultured in Roswell Park Memorial Institute medium (RPMI 1640) supplemented with 10% heat-inactivated fetal bovine serum (FBS). All the cultured cells were maintained in a 37°C with 5% CO_2 incubator.

AuNP synthesis and characterization

AuNPs of 20 nm in diameter were synthesized using the method of citrate reduction of gold salts as previously described.[26] The citrate buffer was removed and AuNPs were coated with FBS before washed and reconstituted in phosphate-buffered saline (PBS). AuNPs were characterized by transmission electron microscopy (TEM) imaging using a Philips CM300FEG system and dynamic light scattering (Malvern Zetasizer Nano ZS).

AuNP treatment

As-synthesized AuNPs were purified via centrifugation to remove the excess citrate buffer and subsequently coated with FBS. The FBS-coated AuNPs were washed and reconstituted in PBS and finally sterile filtered. For the treatment, cells were seeded in six-well cell culture plates with each well containing 2.5×10^5 cells and 1 nmol/L AuNPs in growth media was added to the culture plates the following day (the dose was optimized from the lactate dehydrogenase (LDH) assay and previous studies).[13,26,27]

LDH assay

The Roche Cytotoxicity Detection Kit was used to quantify AuNP-mediated cytotoxicity by measuring the amount of LDH released from the cytosol of damaged SAECs. Briefly, 5000 SAECs per well were seeded into 96-well plate for 24 h. Subsequently, the medium was removed and replaced with 200 μL of medium in each well containing 0, 0.25, 0.5, 0.75, 1 and 2 nmol/L of AuNPs. After 72 h incubation, 100 μL of supernatant were removed and transferred to a new plate. 100 μL of reaction mixture (consisting of a catalyst and dye solution) were then added. After 30 min of incubation at room temperature, the LDH activity in the supernatant was quantified using a Tecan Genios MicroPlate reader at 490 nm wavelength. The experiments were performed in triplicates.

TEM and energy-dispersive X-ray (EDX) microanalysis

SAECs and MRC5 fibroblasts were seeded onto four-chambered coverglass (Lab-Tek™ Chambered Coverglass) and the cells were subjected to 2.5% glutaraldehyde (GA) fixation for 1 h before post-fixation using 1% osmium tetroxide. Dehydration with ascending percentage of alcohol was performed before embedding the samples in araldite. Ultrathin sections were cut and were post-doubly stained with uranyl acetate and lead citrate. Sections were viewed using an Olympus EM208S transmission electron microscope. Elemental analysis was performed under a CM120 BioTWIN electron microscope coupled with a Philips EDAX microanalysis system.

Lipid hydroperoxide (LPO) assay

SAECs were trypsinized and centrifuged at 1000 rotations per minute (rpm) for 5 min. 600 μL of millipore water were added to the pellet and sonicated on ice at 50 amplitude for 40 s with manual pulsing every 10 s using VibracellTM ultrasonic processor (Sonics & Material, CT). LPOs were extracted in chloroform and quantified using Lipid Hydroperoxide Assay Kit (Cayman Chemical Company, MI). Lipid peroxide extraction from sonicated samples using chloroform was done following the manufacturer's instructions. After addition of the chromogen for color development, the samples were aliquoted onto 96-well glass plate and readings were taken in a multi-well plate spectrophotometer.

Alkaline single-cell gel electrophoresis (comet assay)

The SAECs were first embedded in 0.8% low melting agarose (Pronadisa, Spain) on comet slides (Trevigen, MD) and lysed in cold lysis solution (2.5 mol/L NaCl, 0.1 mol/L EDTA, 10 mmol/L Tris base, pH 10) containing 1% Triton X (Trevigen) at 4°C for 1 h. SAECs were denaturated in alkaline buffer (0.3 mol/L NaCl, 1 mmol/L EDTA) for 40 min in the absence of light at room temperature. Electrophoresis at

25 V and 300 mA was performed for 20 min. The slides were then immersed in neutralization buffer (0.5 mol/L Tris-HCl, pH 7.5) for 15 min. Dehydration was achieved using 70% ethanol. Subsequently, the slides were air-dried before stained with SYBR green dye. The tail moments of the SAECs nuclei were measured as an indication of DNA damage. One hundred comets were analyzed per concentration and this was done by using comet imager v1.2 software (Metasystems GmbH).

Trypan blue cell viability counting

50 μL of trypsinized cell suspension were added into 50 μL of 0.4% Trypan blue stain (1 :1 dilution) and mixed well. 10 μL of stained cell suspension were filled to a hemocytometer for cell counting. Under a light microscope, the number of non-viable cells that were stained blue and viable cells that excluded the dye was scored separately. The number of non-viable cells was calculated by multiplying the total number of Trypan blue stained cells by two (the dilution factor for Trypan blue).

Real-time RT-PCR

RNeasy Mini Kit (QIAGEN, Germany) was used to isolate total RNA and purity was measured using NanoDrop® ND-1000 Spectrophometer (Thermo Fisher Scientific, MA) at absorbance reading of 260 and 280 nm wavelength. Cultured monolayers of SAECs and MRC5 cells were lysed, followed by addition of equal volume of 70% ethanol. Samples were then transferred into an RNeasy MinElute Spin Column and centrifuged for 15 s at 13,200 rpm. Samples were subjected to washing steps using RWI and RPE, followed by RNase-free water to elute the RNA. Super ScriptTM III First-Strand Synthesis System for reverse transcription-polymerase chain reaction (RT-PCR) kit (Invitrogen, CA) was used for complementary DNA (cDNA) conversion according to manufacturer's instructions.

The sequences for *MT* isoforms primers used in this study were adapted from Mididoddi *et al.*[28] cDNA was mixed with the SYBR Green PCR Master Mix (Applied Biosystems, CA) and run by a 7900HT Fast Real-Time PCR machine (Applied Biosystems). The thermal profile was set as 95°C, 20 s; 95°C, 1 s followed by 60°C, 20 s for 40 cycles. The *Ct* values were normalized to an endogenous housekeeping gene (glyceraldehyde 3-phosphate dehydrogenase [GAPDH]) where $\Delta Ct = Ct_{\text{sample}} - Ct_{\text{GAPDH}}$. The average values of the ΔCt of the samples were then used to calculate the $\Delta\Delta Ct$ value ($\Delta\Delta Ct = \Delta Ct_{\text{treated}} - \Delta Ct_{\text{control}}$). The fold change in expression for each gene of the samples was calculated by $2^{-\Delta\Delta Ct}$.

Statistical analysis

Values for all experiments are expressed as mean ± standard error (SEM) of three independent experiments. The data were analyzed using Student's *t*-test and one-way analysis of variance (ANOVA) coupled with Tukey post test (Graph Pad Prism Version 5.0 software). $P < 0.05$ was reported statistically significant.

Results

Characteristics of synthesized AuNPs

As characterized by TEM and dynamic light scattering, the mean particle diameter of AuNPs was found to be 22.95 nm in solution, and the size distribution was within 15% of the mean diameter (Figure 1). It was observed that AuNPs induced significant cellular release of LDH at 1 and 2 nmol/L concentrations, indicating cell damage and toxicity (Figure 2). After optimization, 1 nmol/L of AuNPs was selected to treat the cells for further experiment since this dose had been used in our previous studies.[26,27] The 1 nmol/L AuNP concentration used in this study is equivalent to 48.65 μg/mL and falls within the range of AuNP concentrations that are utilized for nanotoxicity studies (as summarized in the review by Khlebtsov and Dykman[10]).

Cellular uptake of AuNPs in SAECs

AuNP agglomerates were found clustered within cytoplasmic vesicles of SAECs as dense, dark spherical deposits (Figure 2a). EDX analysis verified that the electron dense

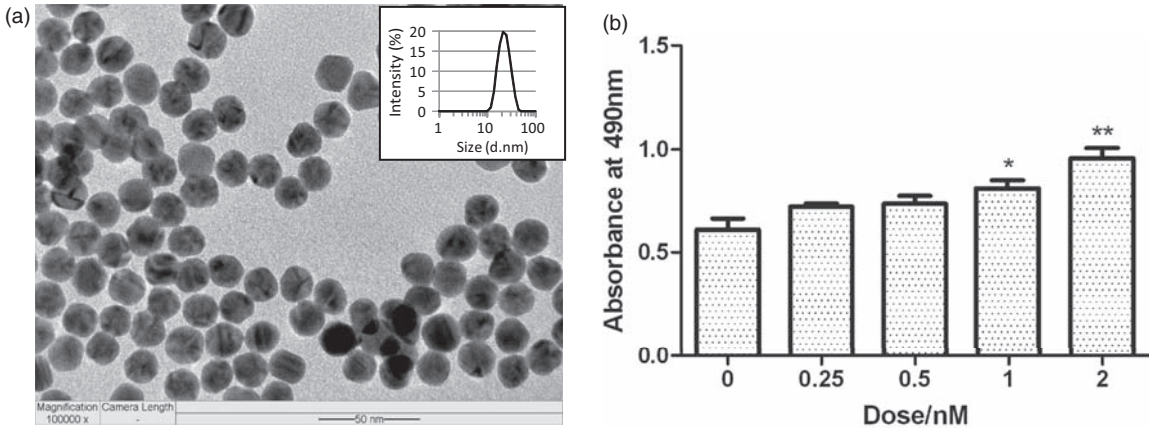

Figure 1 (a) Representative transmission micrograph of synthesized AuNPs (with inset showing size distribution of AuNPs from dynamic light scattering). (b) LDH assay was used to determine cytotoxicity of SAECs treated with a range of dose with AuNPs. All the experiments were conducted in triplicates. Error bars = SEM; *$P < 0.05$; **$P < 0.01$. AuNPs: gold nanoparticles; LDH: lactate dehydrogenase

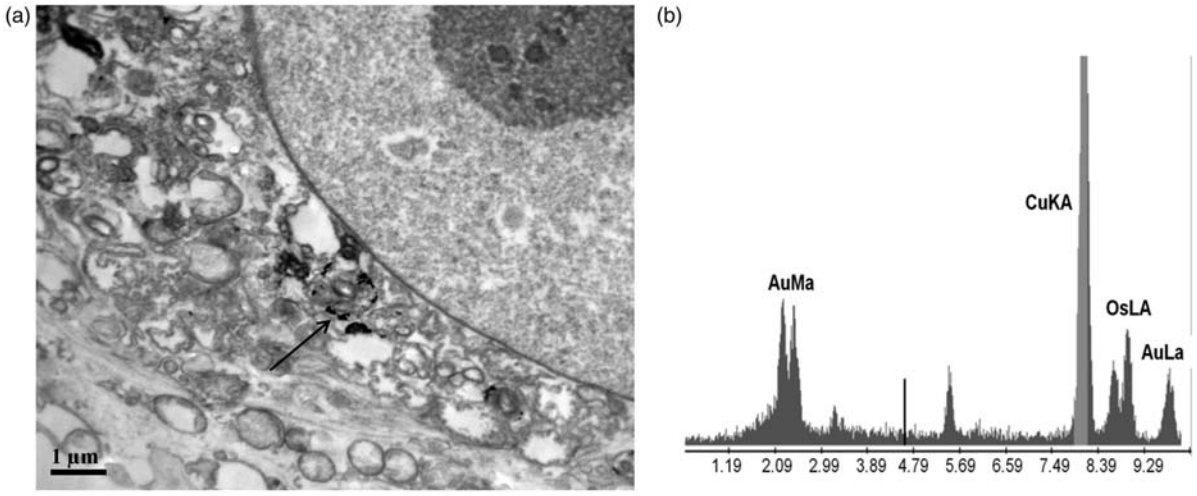

Figure 2 Ultrastructural localization of AuNPs in SAECs by TEM. (a) Micrograph showing the deposition of AuNPs as electron dense deposits (indicated by arrow) in the cytoplasm 72 h after exposure to AuNPs. Scale bar: 1 μm. (b) EDX spectrum showing the presence of Au in SAECs as two sharp peaks at 2.121 and 9.712 keV. AuNPs: gold nanoparticles; EDX: energy-dispersive X-ray; SAECs: small airway epithelial cells; TEM: transmission electron microscopy

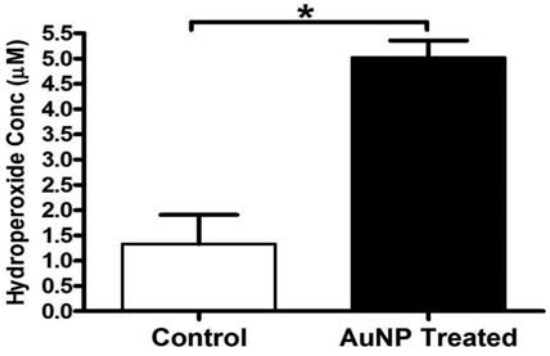

Figure 3 Lipid peroxidative stress in SAECs following exposure to 1 nmol/L AuNPs. A significantly higher level of LPOs was observed in AuNP-treated SAECs when compared with control cells. AuNPs: gold nanoparticles; SAECs: small airway epithelial cells; LPO: lipid hydroperoxide

aggregates are AuNPs as depicted by the presence of two peaks that represent the gold M and L shells with a peak over background (P/B) ratio of 59.80 (Figure 2b). The copper peaks observed were due to the use of copper grids for sample mounting while the osmium peak was attributed to the use of osmium tetroxide during sample preparation.

Oxidative stress generated in SAECs after AuNP exposure

LPO is an established marker of oxidative stress.[29] There was a significant increase of the LPO content as observed in SAECs after 72 h of 1 nmol/L AuNP exposure compared with the unexposed cells (Figure 3). This provides evidence that AuNPs were able to induce oxidative stress in SAECs.

Genotoxic and cytotoxic response in SAECs following AuNP exposure

The *in vitro* comet assay revealed heightened oxidative stress-induced DNA fragmentation after 72 h AuNP exposure (Figure 4a). Tail moment, which refers to the percentage of DNA present in the tail multiplied by the length between the center part of head and tail,[30] was significantly greater in 1 nmol/L AuNP-treated SAECs, indicating that a larger extent of DNA fragmentation incurred in AuNP-treated cells. Following these observations, trypan blue assay showed increased cell death in SAECs in response to oxidative stress (Figure 4b).

Modulation of MT isoforms following exposure to AuNPs in lung cell lines

Human *MT* genes are clustered on a single locus on chromosome 16 (16q13)[31] which encodes the 10 functional isoforms of *MT* genes *MT-1A*, *1B*, *1E*, *1F*, *1 G*, *1H*, *1X*, *2A*, *3* and *4*. As the MT-1 and -2 proteins are ubiquitous in tissues while MT-3 was found to be most prominent in the brain and MT-4 in stratified squamous epithelial cells,[28,32–34] only the expression of functional *MT-1* and *MT-2* gene isoforms were assessed initially in SAECs lung epithelial cells (Figure 5a). The *MT-1X* gene (which was the most abundant isoform) expressed by SAECs was significantly down-regulated following exposure to 1 nmol/L AuNPs (Figure 5b). Since AuNPs were previously shown to increase oxidative stress in the same experimental setting in MRC5 lung fibroblasts,[26] we also compared the *MT* isoforms in both lung cell lines following AuNP exposure. *MT-1A, 1 E, 1X* and *2 A* mRNA levels were detected in the control MRC5 lung fibroblasts (Figure 6a) and a significant increase in the *MT-2 A* and *MT-1X* mRNA transcripts was observed in AuNP-treated lung fibroblasts in comparison with untreated fibroblasts (Figure 6c).

Discussion

In this study, AuNPs were found to be taken up by the small airway cells as verified by ultrastructural observation and elemental profiling. Since AuNPs were found to be isolated

in cytoplasmic vesicles, it is likely that the AuNPs were internalized via endocytosis.[35–38] The phenomenon of cellular agglomeration of AuNPs could be due to the outer coating of NPs with serum.[39] Agglomeration is also likely to occur in the majority of engineered NPs due to inherent properties such as high surface activity[40] and high diffusivity.[41,42]

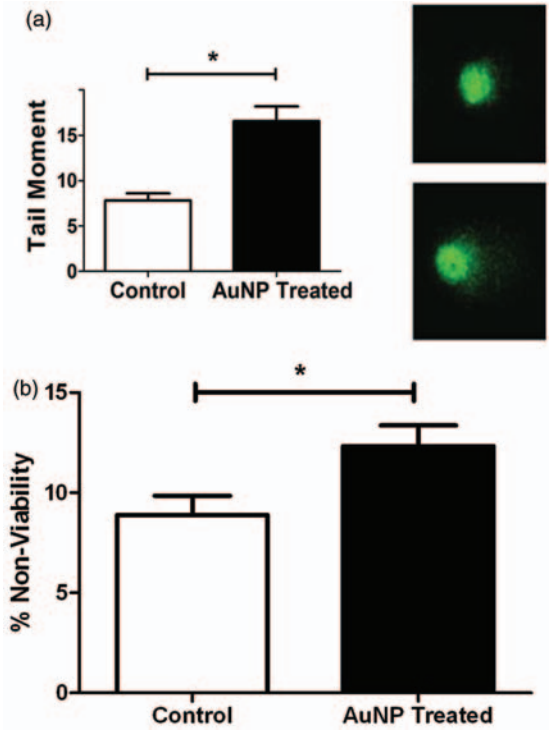

Figure 4 Genotoxic and cytotoxic effects in AuNP-treated SAECs. (a) Comet assay. Cells were treated for 72 h in 1 nmol/L AuNPs and subsequently run on alkaline electrophoresis and stained in SYBR green which visualizes the comet ''tail'', the length of which is an indicator of DNA damage. Analysis of 100 cells per treatment was performed. Control cells (upper right insert) showed little to no tail. AuNP-treated cells (bottom right insert) display a comparatively longer tail, indicative of the presence of higher DNA damage. (b) Viability of SAECs was determined by 0.4% Trypan blue dye exclusion assay following 72 h of 1 nmol/L AuNP exposure. All the experiments were conducted in triplicates. Error bars = SEM; $^*P < 0.05$. AuNPs: gold nanoparticles; SAECs: small airway epithelial cells; SEM: standard error mean (A color version of this figure is available in the online journal)

When SAECs were treated with 1 nmol/L AuNPs, there was an increase in cellular damage concomitant with lipid peroxidation. This phenomenon is similar to our previous study where we observed an increased oxidative stress accompanied by protective effects of antioxidants upon AuNP exposure in MRC5 human lung fibroblasts.[13,26] Oxidative stress due to the increase in ROS would cause oxidative modification on biomolecules like proteins, lipids and carbohydrates, and could lead to the loss of cell function and eventual cell death. One of the common effects from oxidative damage is the peroxidation of lipids. The oxidation of phospholipids leads to the disruption of the plasma membrane and eventually stimulating signaling pathways for apoptosis.[43] Using different types of NPs,[39,44–47] our current study and other studies have shown that oxidative stress is the major route for metal-based NP-induced genotoxicity.[48] In particular, we observed significant DNA damage by the Comet Assay in SAECs exposed to 1 nmol/L of AuNPs showing the DNA damaging potential of AuNPs. Other investigators have also observed the presence of genotoxicity induced by other types of NPs.[39,49–53]

MT is a multi-functional protein that confers cytoprotection in presence of cell insults.[54] MT plays an important role in detoxifying heavy metals and as scavengers of oxidative free radicals.[24] In this study, we observed that exposure of SAECs to 1 nmol/L AuNPs led to down-regulation of the *MT-1X* gene but up-regulation of the *MT-2A* and *MT-1X* genes in the lung fibroblasts. These findings appear to suggest that MT responses may be cell-type specific.[10,39] This could also possibly explain partially why AuNPs affect only cell proliferation in MRC5 lung fibroblasts as reported in our previous study[26] but induce cell damage in SAECs. Down-regulation of MTs has been reported to induce growth arrest and apoptosis in cancer cells.[55] MTs have also been observed to prevent death in cardiac cells by attenuating ER stress.[56] *In vivo* experiments have revealed that MT is most effective in the quenching of free radicals as compared with other sulfhydryl molecules with MT-2 being six-fold more effective in scavenging free radicals than MT-1.[57] The same study also demonstrated that MTs and MT-like proteins isolated from mouse brains could

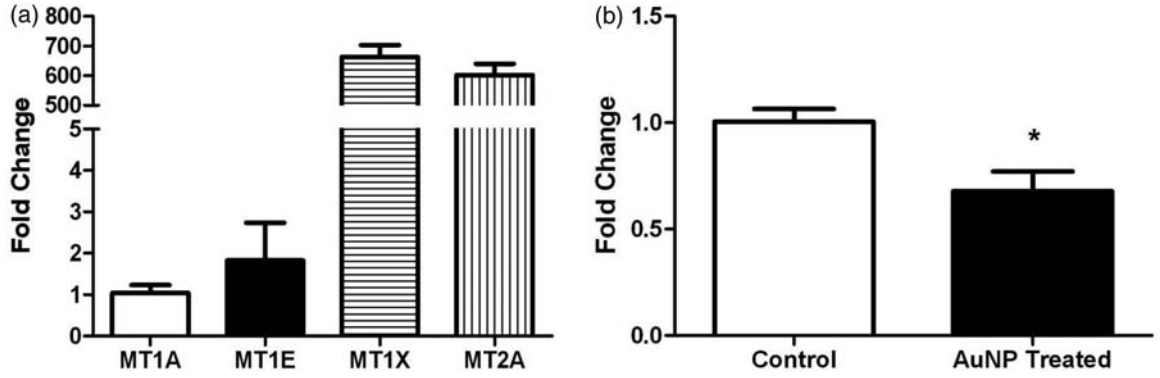

Figure 5 MT expression in control and AuNP-treated SAECs. (a) Bar chart of *MT* isoforms that was present endogenously in SAECs. (b) Significant difference in fold change of the *MT-1X* gene in SAECs was observed after treatment with 1 nmol/L AuNPs. Error bars = SEM; $^*P < 0.05$. AuNPs: gold nanoparticles; MT: metallothionein; SAECs: small airway epithelial cells; SEM: standard error mean

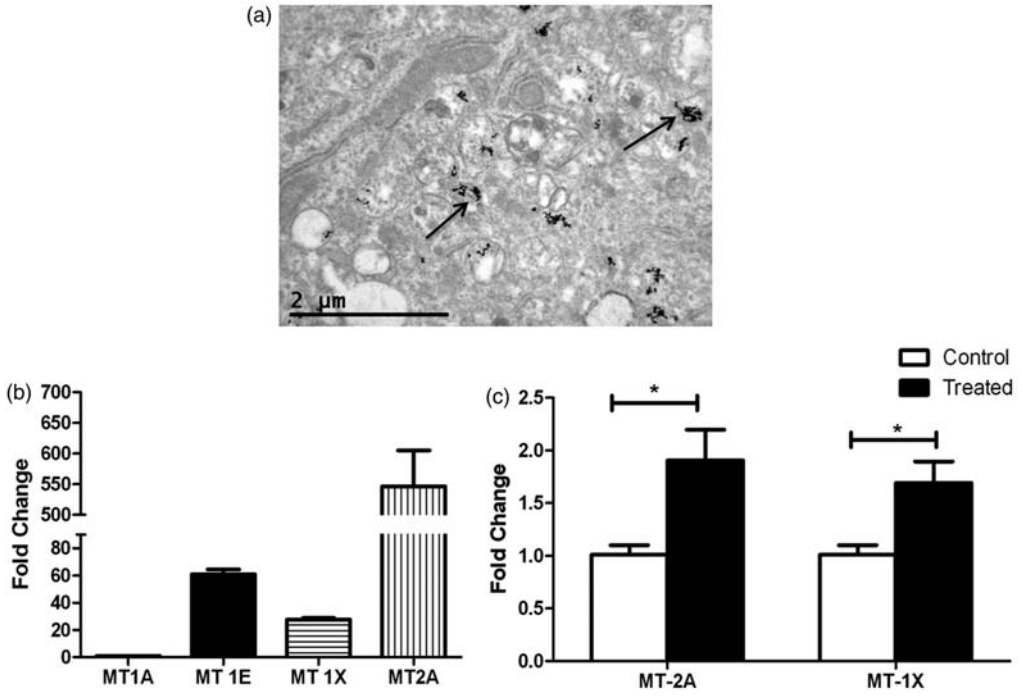

Figure 6 MT expression in control and AuNP-treated MRC lung fibroblasts. (a) Mircograph showing deposition of AuNPs (indicated by arrows) in MRC5 cells. Scale bar = 2 µm. (b) Bar chart of *MT* isoforms endogenously expressed in MRC5 cells, with *MT-2 A* showing the highest expression. (c) Significant up-regulation of *MT-2 A* and *MT-1X* after exposure to 1 nmol/L AuNPs. All the experiments were conducted in triplicates. Error bars = SEM; $^*P < 0.05$. AuNPs: gold nanoparticles; MT: metallothionein; SEM: standard error mean.

scavenge superoxide radicals and exert neuroprotective effects.

In summary, 1 nmol/L AuNPs induced significant cytotoxicity and genotoxicity with concomitant oxidative stress in lung epithelial cells *in vitro*, accompanied by altered expression of *MT* genes which is dependent on the cell type. More extensive studies would need to be conducted *in vivo* to verify the safety issues related to increased applications of AuNPs in consumer, industrial and biomedical applications.

Author contributions: CTN and JJL conducted the experiments and performed the data analysis. CTN drafted the manuscript. RLG and MPH were involved in Comet assay. BHB and LYLY provided input to the experimental design and protocols, and made amendments to the manuscript. CNO provided scientific comments and suggestions. All authors have read the manuscript before submission.

ACKNOWLEDGMENTS

This study was supported by the Singapore Ministry of Education Academic Research Fund Tier 2 Grant Number MOE2008-T2-1-046. Our appreciation goes to Dr. Deny Hartono from the Department of Chemical and Biomolecular Engineering for his assistance in synthesizing gold nanoparticles used in this study.

REFERENCES

1. Warheit DB, Sayes CM, Reed KL, Swain KA. Health effects related to nanoparticle exposures: environmental, health and safety considerations for assessing hazards and risks. *Pharmacol Ther* 2008;**120**:35–42
2. Griffitt RJ, Hyndman K, Denslow ND, Barber DS. Comparison of molecular and histological changes in zebrafish gills exposed to metallic nanoparticles. *Toxicol Sci* 2009;**107**:404–15
3. United States Environmental Protection Agency. See http://www.epa.gov/nanoscience/ (last checked 17 January 2013)
4. Powell MC, Kanarek MS. Nanomaterial health effects–part 1: background and current knowledge. *WMJ* 2006;**105**:16–20
5. Powell MC, Kanarek MS. Nanomaterial health effects–Part 2: uncertainties and recommendations for the future. *WMJ* 2006;**105**:18–23
6. Sandhu KK, McIntosh CM, Simard JM, Smith SW, Rotello VM. Gold nanoparticle-mediated transfection of mammalian cells. *Bioconjug Chem* 2002;**13**:3–6
7. Dreaden EC, Mackey MA, Huang X, Kang B, El-Sayed MA. Beating cancer in multiple ways using nanogold. *Chem Soc Rev* 2011;**40**:3391–404
8. Nowack B, Bucheli T. Occurrence, behavior and effects of nanoparticles in the environment. *Environ Pollut* 2007;**150**:5–22
9. Singh N, Manshian B, Jenkins GJ, Griffiths SM, Williams PM, Maffeis TG, Wright CJ, Doak SH. NanoGenotoxicology: the DNA damaging potential of engineered nanomaterials. *Biomaterials* 2009;**30**:3891–914
10. Khlebtsov N, Dykman L. Biodistribution and toxicity of engineered gold nanoparticles: a review of in vitro and in vivo studies. *Chem Soc Rev* 2011;**40**:1647–71
11. Muller J, Huaux F, Fonseca A, Nagy JB, Moreau N, Delos M, Raymundo-Piñero E, Béguin F, Kirsch-Volders M, Fenoglio I, Fubini B, Lison D. Structural defects play a major role in the acute lung toxicity of multiwall carbon nanotubes: toxicological aspects. *Chem Res Toxicol* 2008;**21**:1698–705
12. van der Zande M, Junker R, Walboomers XF, Jansen JA. Carbon nanotubes in animal models: a systematic review on toxic potential. *Tissue Eng Part B Rev* 2011;**17**:57–69
13. Li JJ, Hartono D, Ong CN, Bay BH, Yung LY. Autophagy and oxidative stress associated with gold nanoparticles. *Biomaterials* 2010;**31**:5996–6003
14. Han SG, Newsome B, Hennig B. Titanium dioxide nanoparticles increase inflammatory responses in vascular endothelial cells. *Toxicology* 2013;**306**:1–8

15. Skocaj M, Filipic M, Petkovic J, Novak S. Titanium dioxide in our everyday life; is it safe? *Radiol Oncol* 2011;**45**:227–47
16. Hext PM, Tomenson JA, Thompson P. Titanium dioxide: inhalation toxicology and epidemiology. *Ann Occup Hyg* 2005;**49**:461–72
17. Maynard AD, Warheit DB, Philbert MA. The new toxicology of sophisticated materials: nanotoxicology and beyond. *Toxicol Sci* 2011;**120**(Suppl 1): S109–29
18. Johnston HJ, Hutchison G, Christensen FM, Peters S, Hankin S, Stone V. A review of the in vivo and in vitro toxicity of silver and gold particulates: particle attributes and biological mechanisms responsible for the observed toxicity. *Crit Rev Toxicol* 2010;**40**:328–46
19. Srinivas A, Rao PJ, Selvam G, Murthy PB, Reddy PN. Acute inhalation toxicity of cerium oxide nanoparticles in rats. *Toxicol Lett* 2011;**205**:105–15
20. Chompoosor A, Saha K, Ghosh PS, Macarthy DJ, Miranda OR, Zhu ZJ, Arcaro KF, Rotello VM. The role of surface functionality on acute cytotoxicity, ROS generation and DNA damage by cationic gold nanoparticles. *Small* 2010;**6**:2246–49
21. Pan Y, Leifert A, Ruau D, Neuss S, Bornemann J, Schmid G, Brandau W, Simon U, Jahnen-Dechent W. Gold nanoparticles of diameter 1.4 nm trigger necrosis by oxidative stress and mitochondrial damage. *Small* 2009;**5**:2067–76
22. Borm PJ, Kreyling W. Toxicological hazards of inhaled nanoparticles–potential implications for drug delivery. *J Nanosci Nanotechnol* 2004;**4**:521–31
23. Vallee BL. The function of metallothionein. *Neurochem Int* 1995;**27**:23–33
24. Cherian MG, Jayasurya A, Bay BH. Metallothioneins in human tumors and potential roles in carcinogenesis. *Mutat Res* 2003;**533**:201–9
25. Saito S, Kojima Y. Relative gold-binding capacity of metallothionein: studies in renal cytosols of gold-injected rats. *Res Commun Mol Pathol Pharmacol* 1996;**92**:119–26
26. Li JJ, Zou L, Hartono D, Ong CN, Bay BH, Yung LY. Gold nanoparticles induce oxidative damage in lung fibroblasts in vitro. *Adv Mater* 2008;**20**:138–42
27. Li JJ, Lo SL, Ng CT, Gurung RL, Hartono D, Hande MP, Ong CN, Bay BH, Yung LY. Genomic instability of gold nanoparticle treated human lung fibroblast cells. *Biomaterials* 2011;**32**:5515–23
28. Mididoddi S, McGuirt JP, Sens MA, Todd JH, Sens DA. Isoform-specific expression of metallothionein mRNA in the developing and adult human kidney. *Toxicol Lett* 1996;**85**:17–27
29. Potter TM, Neun BW, Stern ST. Assay to detect lipid peroxidation upon exposure to nanoparticles. *Methods Mol Biol* 2011;**697**:181–9
30. Olive PL, Banath JP, Durand RE. Heterogeneity in radiation-induced DNA damage and repair in tumor and normal cells measured using the ''comet'' assay. *1990.* Radiat Res 2012;**178**:AV35–42
31. Karin M, Eddy RL, Henry WM, Haley LL, Byers MG, Shows TB. Human metallothionein genes are clustered on chromosome 16. *Proc Natl Acad Sci U S A* 1984;**81**:5494–8
32. Vasak M, Hasler DW. Metallothioneins: new functional and structural insights. *Curr Opin Chem Biol* 2000;**4**:177–83
33. Stennard FA, Holloway AF, Hamilton J, West AK. Characterisation of six additional human metallothionein genes. *Biochim Biophys Acta* 1994;**1218**:357–65
34. West AK, Stallings R, Hildebrand CE, Chiu R, Karin M, Richards RI. Human metallothionein genes: structure of the functional locus at 16q13. *Genomics* 1990;**8**:513–18
35. Khan JA, Pillai B, Das TK, Singh Y, Maiti S. Molecular effects of uptake of gold nanoparticles in HeLa cells. *Chembiochem* 2007;**8**:1237–40
36. Chithrani DB. Intracellular uptake, transport, and processing of gold nanostructures. *Mol Membr Biol* 2010;**27**:299–311
37. Wang SH, Lee CW, Chiou A, Wei PK. Size-dependent endocytosis of gold nanoparticles studied by three-dimensional mapping of plasmonic scattering images. *J Nanobiotechnol* 2010;**8**:33
38. Zhang Q, Hitchins VM, Schrand AM, Hussain SM, Goering PL. Uptake of gold nanoparticles in murine macrophage cells without cytotoxicity or production of pro-inflammatory mediators. *Nanotoxicology* 2011;**5**:284–95
39. Shukla RK, Sharma V, Pandey AK, Singh S, Sultana S, Dhawan A. ROS-mediated genotoxicity induced by titanium dioxide nanoparticles in human epidermal cells. *Toxicol In Vitro* 2011;**25**:231–41
40. Kim S, Choi JE, Choi J, Chung KH, Park K, Yi J, Ryu DY. Oxidative stress-dependent toxicity of silver nanoparticles in human hepatoma cells. *Toxicol In Vitro* 2009;**23**:1076–84
41. Gosens I, Post JA, de la Fonteyne LJ, Jansen EH, Geus JW, Cassee FR, de Jong WH. Impact of agglomeration state of nano- and submicron sized gold particles on pulmonary inflammation. *Part Fibre Toxicol* 2010;**7**:37
42. Wong BA, Nash DG, Moss OR. Generation of nanoparticles agglomerates and their dispersion in lung serum simulant or water. *J Phys Conf Ser* 2009;**151**:012036
43. Ryter SW, Kim HP, Hoetzel A, Park JW, Nakahira K, Wang X, Choi AM. Mechanisms of cell death in oxidative stress. *Antioxid Redox Signal* 2007;**9**:49–89
44. Schins RP, Knaapen AM. Genotoxicity of poorly soluble particles. *Inhal Toxicol* 2007;**19**(Suppl 1): 189–98
45. Jin CY, Zhu BS, Wang XF, Lu QH. Cytotoxicity of titanium dioxide nanoparticles in mouse fibroblast cells. *Chem Res Toxicol* 2008;**21**:1871–7
46. Reeves JF, Davies SJ, Dodd NJ, Jha AN. Hydroxyl radicals (*OH) are associated with titanium dioxide (TiO(2)) nanoparticle-induced cytotoxicity and oxidative DNA damage in fish cells. *Mutat Res* 2008;**640**:113–22
47. Lu S, Duffin R, Poland C, Daly P, Murphy F, Drost E, Macnee W, Stone V, Donaldson K. Efficacy of simple short-term in vitro assays for predicting the potential of metal oxide nanoparticles to cause pulmonary inflammation. *Environ Health Perspect* 2009;**117**:241–7
48. Yang H, Liu C, Yang D, Zhang H, Xi Z. Comparative study of cytotoxicity, oxidative stress and genotoxicity induced by four typical nanomaterials: the role of particle size, shape and composition. *J Appl Toxicol* 2009;**29**:69–78
49. Johnston HJ, Hutchison GR, Christensen FM, Aschberger K, Stone V. The biological mechanisms and physicochemical characteristics responsible for driving fullerene toxicity. *Toxicol Sci* 2010;**114**:162–82
50. Naqvi S, Samim M, Abdin M, Ahmed FJ, Maitra A, Prashant C, Dinda AK. Concentration-dependent toxicity of iron oxide nanoparticles mediated by increased oxidative stress. *Int J Nanomed* 2010;**5**:983–9
51. Petkovic J, Zegura B, Stevanovic M, Drnovsek N, Uskokovic D, Novak S, Filipič M. DNA damage and alterations in expression of DNA damage responsive genes induced by TiO(2) nanoparticles in human hepatoma HepG2 cells. *Nanotoxicology* 2011;**5**:341–53
52. Guo YY, Zhang J, Zheng YF, Yang J, Zhu XQ. Cytotoxic and genotoxic effects of multi-wall carbon nanotubes on human umbilical vein endothelial cells in vitro. *Mutat Res* 2011;**721**:184–91
53. Lee K, Lee H, Lee KW, Park TG. Optical imaging of intracellular reactive oxygen species for the assessment of the cytotoxicity of nanoparticles. *Biomaterials* 2011;**32**:2556–65
54. Tanaka S, Niioka T. Cytoprotective effects of metallothionein induced by metals against oxidative stress induced by hydrogen peroxide. *Biomed Res Trace Elem* 2001;**12**:353–4
55. Li J, Liu Y, Ru B. Effect of metallothionein on cell viability and its interactions with cadmium and zinc in HEK293 cells. *Cell Biol Int* 2005;**29**:843–8
56. Xu J, Wang G, Wang Y, Liu Q, Xu W, Tan Y, Cai L. Diabetes- and angiotensin II-induced cardiac endoplasmic reticulum stress and cell death: metallothionein protection. *J Cell Mol Med* 2009;**13**:1499–512
57. Hussain S, Slikker Jr W, Ali SF. Role of metallothionein and other antioxidants in scavenging superoxide radicals and their possible role in neuroprotection. *Neurochem Int* 1996;**29**:145–52

(Received March 18, 2013, Accepted August 1, 2013)